Chalcogenide Letters Vol. 10, No. 3, March 2013, p. 121 - 129

THERMOLUMINESCENCE STUDIES OF $SrAl_2O_4$: Eu PHOSPHORS AT DIFFERENT DY CONCENTRATIONS

D. S. KSHATRI[a], AYUSH KHARE[a*], PIYUSH JHA[b]
[a]*Department of Physics,National Institute of Technology, G E Road, Raipur – 492 010 India*
[b]*Department of P. G. Studies and Research in Physics, R. D. University, Jabalpur - 482 001 India*

$Sr(NO_3)_2$, $Al(NO_3)_3$, NH_2CONH_2, Eu_2O_3 and Dy_2O_3 are used as the raw materials for the preparation of $SrAl_2O_4$ (RE: Eu, Dy) precursor by the combustion synthesis technique (CST), which is widely known to prepare nano sized phosphors. The influence of varied concentration of Dy on crystal structure and optical properties is analyzed by means of X-ray diffraction (XRD), scanning electron microscopy (SEM) and thermoluminescence (TL) spectra. The fine flake-like phosphors with reasonable good brightness and long afterglow are obtained by treating the samples at different temperatures. XRD patterns reveal a dominant phase characteristics of the monoclinic $SrAl_2O_4$ compound and the presence of dopants having uncognizable effect on the basic crystal structure of $SrAl_2O_4$. From XRD studies, the average particle size of the flake-like $SrAl_2O_4$: Eu, Dy phosphors is calculated to be nearly 12 nm. The optical properties in terms of TL glow curves are studied and discussed systematically. The results indicate that the peak positions in the spectra are not much affected by varying concentration of Dy. The different parameters like activation energy, frequency factor and shape factor are calculated using TL glow curves.

(Received February 7, 2013; Accepted March 15, 2013)

Keywords: Phosphors, optical properties, thermoluminescence, XRD, SEM

1. Introduction

In recent years, the strontium aluminates have attracted intense research around the world, as they offer excellent properties such as high quantum efficiency, long persistence of phosphorescence and good stability. Also, the importance of rare earth ions as efficient emitter in a variety of solid-state matrices is well known. Among rare earth ions, Eu/Dy is often employed by researchers for making red emitting phosphors, where the prominent 612 nm emission band arises from electric dipole moment allowed transitions [1]. The long lasting phosphors (LLP) oxide materials have been developed to replace the conventional sulfide afterglow materials because of their improved luminescent properties such as high initial brightness, long lasting time, suitable emission color and satisfactory chemical stability [2–4], which result in an unexpectedly large field of applications e.g. luminous paints in highways, airports, buildings and ceramic products [5]. These oxide phosphors exhibit a long period of luminescence after an initial rapid attenuation, and the lasting time of this new kind of phosphors is more than 10 times than that of sulfide phosphors [6]. $SrAl_2O_4:Eu^{2+}$, Dy^{3+} as one of the persistent luminescence materials, has been studied extensively because it is the brightest LLP emitter found [7]. In addition to a higher chemical stability, the intensity and the duration of the phosphorescence of strontium aluminates (especially $SrAl_2O_4:Eu^{2+}$, Dy^{3+}) makes it possible to envisage a continuous light emission during a whole

*Corresponding author:akhare.phy@nitrr.ac.in

night (10 h), hence greatly renewing interests in the phosphorescence phenomenon. In most reports, the oxide LLP materials with large size are prepared using solid-state reaction [8] technique and in order to obtain much smaller particles, the larger phosphor particles need to be grinded further, which can easily introduce additional defects and greatly reduce the luminescence efficiency [9]. With the development of newer technologies, several kinds of chemical synthesis techniques such as co-precipitation [10], sol–gel [11], reverse micro emulsion [12] and combustion methods [13-14] have been employed to prepare $SrAl_2O_4$ and its phosphors. Comparatively speaking, above methods are suitable to synthesize the phosphor with smaller sizes but often difficult to achieve well-defined morphologies. The optical properties of luminescent materials not only are closely related to its native crystal structure but also to its morphology. Therefore, exploring new methods for controlled synthesis of $SrAl_2O_4$: Eu^{+2}, Dy^{3+} with well defined morphology and studying morphology dependent properties become a subject of investigation [15]. Among these, CST has been an interesting method for preparing precursor powders [16]. This synthesis technique uses the heat energy released by the redox exothermic reaction between the metal nitrates and urea or other fuels at a relatively low-igniting temperature. The process is not only safe but also time and energy saving [17]. Many materials have been prepared by using this process, for example, nano-$SrAl_2O_4$:Eu^{2+} was prepared using metal nitrate–urea system [14] and nano-$SrAl_2O_4$:Eu^{2+},Dy^{3+} was prepared by using metal nitrate–glycine solution system [13]. Many aluminates are similar to gallates in structure and properties and have been investigated and used as photoluminescence (PL), cathodoluminescence (CL) and recently plasma display panel (PDP) phosphors for their high quantum efficiency in the visible region [18-19]. Bright green colour electroluminescence (EL) emission has been obtained from $ZnAl_2O_4$: Mn [20]. Therefore, aluminates may be potential phosphors for various applications.

The CST has been investigated as a tool to produce homogenous, crystalline, fine oxide powders as an alternative to time-consuming solid-state reaction and sol-gel processing techniques. For the synthesis of aluminium based oxide phosphors, this method is widely accepted nowadays. Several reports are available on the synthesis of different strontium family hosts such as $Sr_3Al_2O_6$, $Sr_4Al_{14}O_{25}$, $SrAl_2O_4$ and $SrAl_{12}O_{19}$ using low temperature combustion but as far as known to us the effects of co-dopant concentration on persistent TL have not been investigated much. In the present paper, we report preparation, characterization and optical properties of $Sr_{(1-x)}Al_2O_4$: $Eu^{2+}_{0.01}$, Dy_x^{3+} (x = 0.01, 0.02, 0.03) phosphors at varied concentration of Dy as dopant using CST.

2. Experimental details

2.1. Sample preparation

For preparing powder samples, stoichiometric amounts of strontium nitrate [Sr $(NO_3)_2$], aluminum nitrate [Al $(NO_3)_3.9H_2O$] and urea [CO $(NH_2)_2$] (All AR grade, 99.9% pure) weighed using Shimadzu ATX 224 single pan analytical balance are used as raw materials. In addition to it, europium oxide (Eu_2O_3) and dysprosium oxide (Dy_2O_3) taken as co-activators are dissolved in concentrated nitric acid (HNO_3) before transferring them to crucible. The small amount of boric acid (H_3BO_3) is used as the flux while the urea [CO $(NH_2)_2$] is used as fuel. A crucible is used as a container within which chemical reaction takes place. After the solution is transferred into the crucible with comparatively larger volume, it is placed into a furnace already maintained at a temperature of 600℃. Within 5 minutes, the furnace reaches the desired temperature and reaction starts giving yellowish flame. This continues for next few seconds and as it is over, crucible is taken out of the furnace and kept in open to allow cooling. The mixture froths and swells forming foam, which ruptures with a flame and glows to incandescence. Upon cooling, we get fluffy form of material, which is then crushed using agate pestle mortar (diameter-5") to get material in the powder form (Fig.1).

$$2\ Al\ (NO_3)_3.\ 9H_2O + Sr\ (NO_3)_2 + 6CO\ (NH_2)_2 \rightarrow SrAl_2O_4 + 16O_2 + 20\ NH_3 + 6CO_2$$

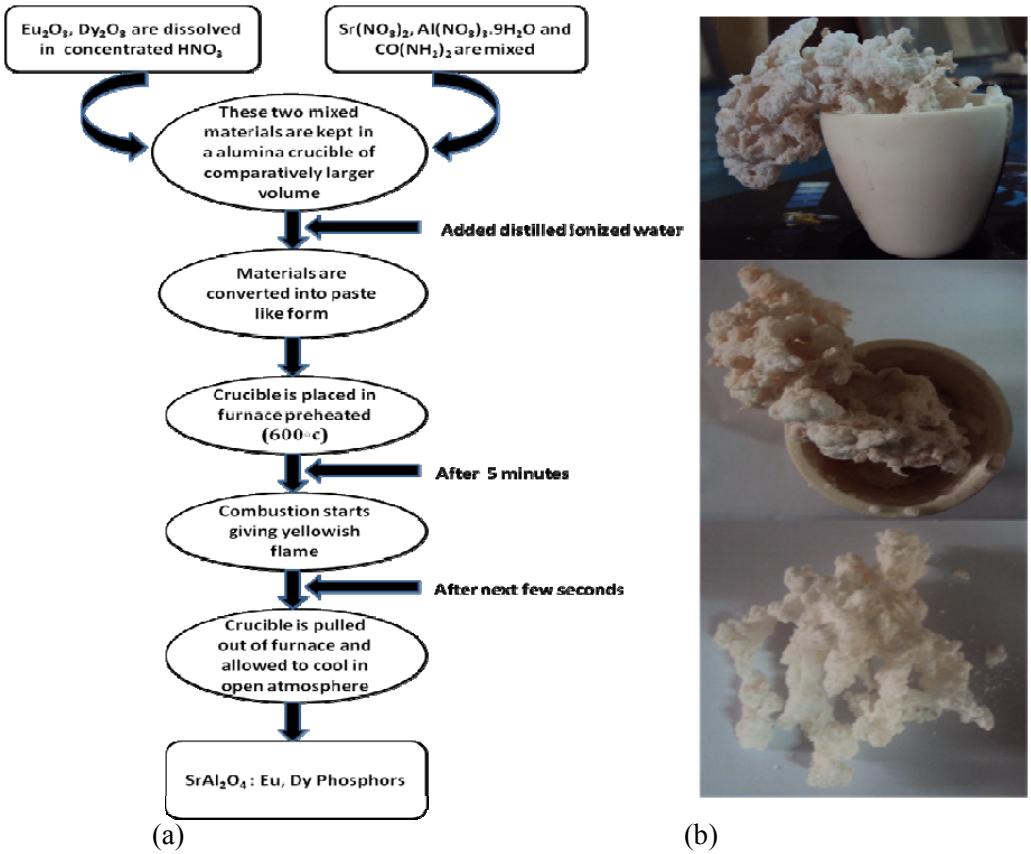

Fig.1 Schematic diagram showing synthesis of $SrAl_2O_4$: Eu, Dy phosphors via combustion method

2.2. Measuring instruments

The materials are weighed using Shimadzu ATX 224 single pan analytical balance and the samples are prepared in a digital furnace already maintained a temperature of 600 ^{o} C. The crystalline structure, size and phase composition of the sample are examined by Rigaku Miniflex II using Cu-Kα radiation (λ=1.5406 A^{o}), where X-rays are generated at 30 KV/15 mA voltage and current values respectively. The morphology of as prepared samples is studied using JEOL JSM-6380 scanning electron microscope (SEM). The TL spectra at different temperatures are recorded using Nucleonics make TL reader (model I 1009 h), where samples are excited with UV radiation at 365 nm wavelength. The heating is performed from room temperature (RT) upto 400 ^{o}C and heating rate under thermal stimulation is varied 3 ^{o}C/s.

3. Results and discussion

3.1. Characterization

Morphology

The SEM study is carried out to investigate the surface morphology and the average crystallite size of the synthesized phosphors. Fig. 2 shows the representative SEM micrographs taken for $SrAl_2O_4$: Eu phosphors at different Dy concentrations. Generally the particles are of irregular shape with voids and flakes [21] distributed all over. For Eu doped precursor, non-uniformly distributed flake type structures are seen, which improve slightly upon addition of Dy in different ratios. In Dy doped samples the crystallites are seen to be uniformly distributed and the voids are occupied. The reason for lots of vacant space may be that the mixture containing stoichiometric amount of redox mixture when heated rapidly at 600^{o}C boils and undergoes dehydration followed by decomposition generating combustile gases such as oxides of N_2, H_2O and nascent oxygen. The volatile combustile gases ignite and burn with a flame and

provide conditions for formation of phosphor lattice with dopants. The large amount of escaping gases dissipates heat and thereby prevents the material from sintering and provides conditions for formation of nano crystalline phase. Also, as the gases escape they leave voluminous, foaming and crystalline fine powder occupying the entire volume of the firing container and have no chance of forming agglomeration unlike in other conventional process [22]. In the samples with greater concentrations of Dy, some layer type growth is visible, which is an indicative of more intensity and high degree of hardness in these samples as is evident from TL studies. It is noticed that the average crystallite size varies in nanometer range. The crystallites have sharp surface morphology of crystalline grains. The exothermicity of the redox reaction between metal nitrates and fuel allows the generation and transport of large amount of heat within the reaction chamber, which couples with the driving force (a difference in chemical potential) and causes the system to depart from its equilibrium state. The interface is a unique place where the crystal grows and is atomically rough when the growth takes place from the melt phase as in case of combustion where the precursor solution initially melts before producing the combustion flame.

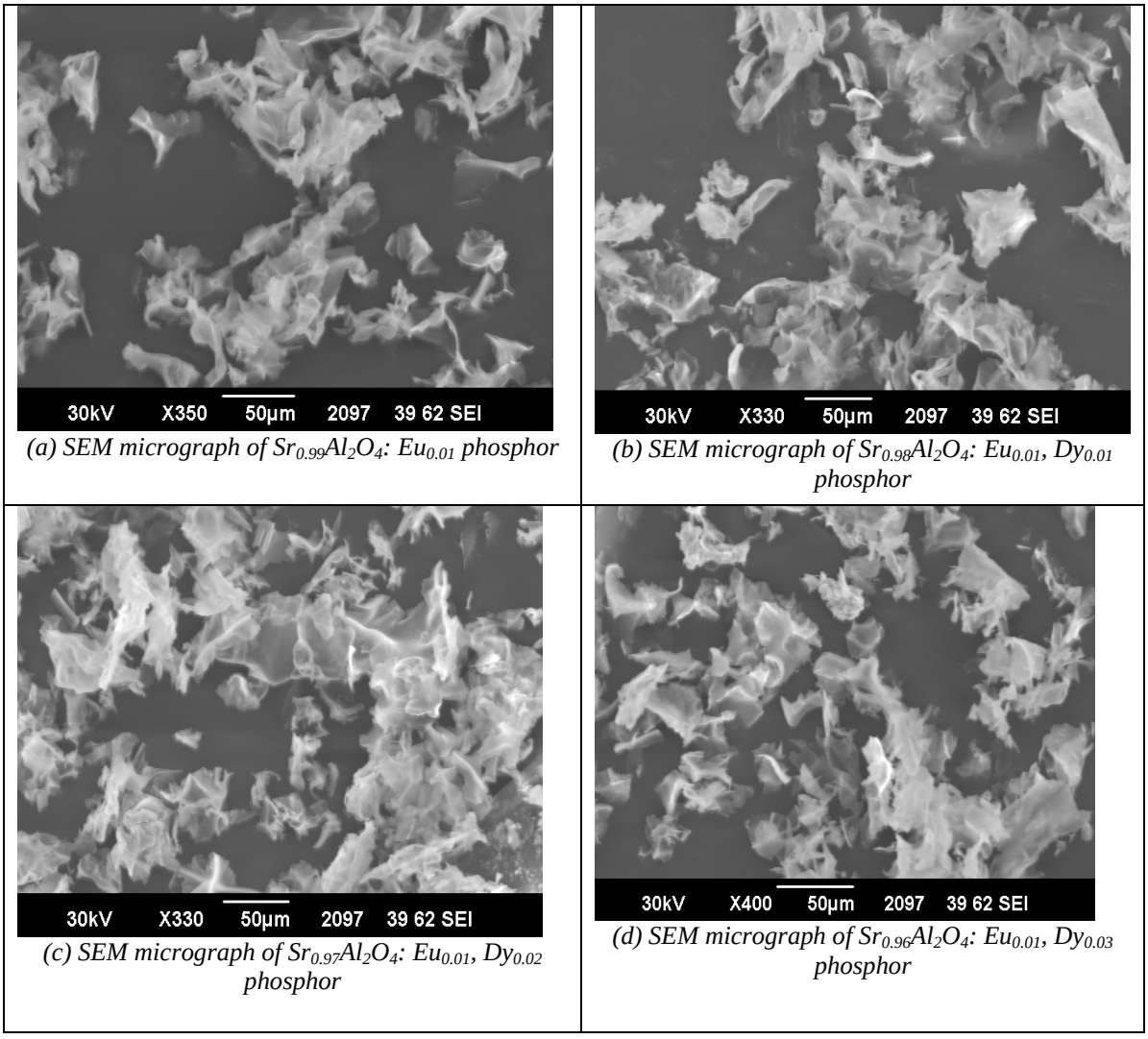

(a) SEM micrograph of $Sr_{0.99}Al_2O_4$: $Eu_{0.01}$ phosphor

(b) SEM micrograph of $Sr_{0.98}Al_2O_4$: $Eu_{0.01}$, $Dy_{0.01}$ phosphor

(c) SEM micrograph of $Sr_{0.97}Al_2O_4$: $Eu_{0.01}$, $Dy_{0.02}$ phosphor

(d) SEM micrograph of $Sr_{0.96}Al_2O_4$: $Eu_{0.01}$, $Dy_{0.03}$ phosphor

Fig. 2

X-ray diffraction (XRD)

The XRD is used to confirm the crystalline nature of the as synthesized host phosphor and to identify the presence of any impurity phases of compositions different from host material. The analysis of XRD data of $SrAl_2O_4$ phases is usually qualitative, just based on relative peak

intensities. The typical X-ray diffraction patterns for combustion synthesized $SrAl_2O_4$: Eu phosphor powders in presence of different Dy concentrations are presented in fig. 3. It is seen that the monoclinic $SrAl_2O_4$ phase pattern is characterized by peaks around $2\theta = 20^o$, 29^o, 34^o, 40^o and 46^o (JCPDS No. 34-0379). An estimation of average crystallite size for the sample is done using Scherrer's formula [23, 24] from the full width at half maximum (FWHM) of the most intense peak at $2\theta = 28{\cdot}46^o$.

$$c.\ s. = K\lambda / \beta \cos\theta \qquad (1)$$

where λ is the wavelength of X-rays employed, β the full width at half maxima (FWHM) of the peak measured in radians, K a constant, which ranges between 0.87 and 1.1 for different crystalline shapes and θ is the Bragg's angle. Here it is important to mention that for calculating average crystallite size, we have used the width of the bunch of reflections at $28{\cdot}46^o$ instead of the single -211 reflection. Otherwise it is difficult to determine it from the present data, because of the modest quality of the diffraction patterns. The average crystallite size using the width of the bunch of reflections is calculated to lie around 12 nm. Also, it is possible that the crystallites are anisotropic so that the diffracting domain size is different in different directions and the width is inversely proportional to the crystallite size. The Table 1 sums up the XRD data in terms of lattice interval, crystallite size, Miller indices etc. The XRD results prove that the phosphors prepared in this work belong to $SrAl_2O_4$ phase mainly, and the co-doped Eu and Dy ions do not have much influence on the crystal structure of luminescent material. Except variations in intensities, the addition of dopant ions has no significant contribution on the host matrix due to the similar ionic radii. The peaks in XRD patterns of different samples are similar to each other and are attributed to $SrAl_2O_4$ monoclinic phase. Actually, there are two phases in $SrAl_2O_4$, a low temperature monoclinic phase and a high temperature hexagonal phase [25] and the transition takes place at 650^oC [26].

Table 1 XRD data of Dy doped $SrAl_2O_4$: Eu phosphor

2 Theta (radian)	**Intensity (Arb. Unit)**	**fwhm (β) (radian)**	**Crystallite size (nm)**	**Lattice spacing (A^o)**	**h k l**
19.48	823.85	0.58	9.19	4.56	(011)
28.46	1298.96	2.08	3.92	3.13	(-211)
34.31	1157.05	1.08	11.89	2.61	(002)
40.04	784.04	2.77	5.07	2.25	(031)
46.07	673.88	2.01	5.51	1.97	(400)

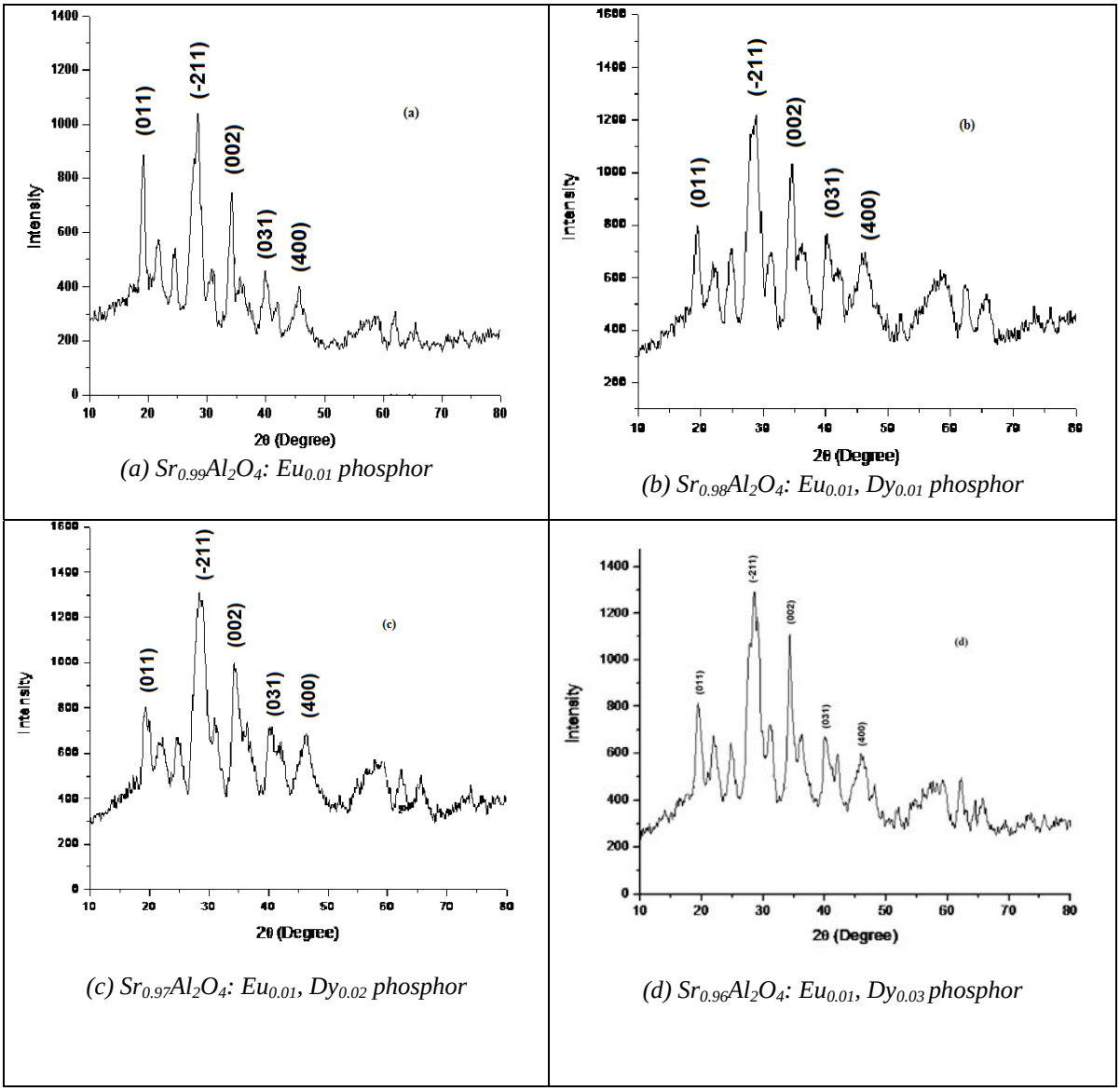

(a) $Sr_{0.99}Al_2O_4$: $Eu_{0.01}$ phosphor

(b) $Sr_{0.98}Al_2O_4$: $Eu_{0.01}$, $Dy_{0.01}$ phosphor

(c) $Sr_{0.97}Al_2O_4$: $Eu_{0.01}$, $Dy_{0.02}$ phosphor

(d) $Sr_{0.96}Al_2O_4$: $Eu_{0.01}$, $Dy_{0.03}$ phosphor

Fig. 3 X-ray diffractogram of phosphor

3.2 TL Studies

TL is the thermally stimulated emission of light following the absorption of energy from radiations. The radiations cause displacement of electrons within the crystal lattice of the substance. Upon heating, the trapped electrons return to their normal, lower-energy positions, releasing energy in the process. TL is an effective tool for various applications, namely, dosimetry, in biological applications, age determination, geology or solid state defect structure analysis, etc. The main objective of TL experiments is to extract data from an experimental glow curve, or a series of glow curves, and to use these data to calculate values for the various parameters associated with the luminescence processes involved. These parameters include the activation energy, frequency factor, order of kinetics and shape factor in energy space. The TL properties measured in a short period are indicative of emission intensity and afterglow lifetime, which are helpful to estimate longtime luminescence. $SrAl_2O_4$: Eu, Dy phosphors are known to exhibit photoconductivity under ultraviolet and X-ray irradiation [27]. Actually the Eu^{2+} $4f^7$ ground energy state is 3.2 eV below the bottom of the conduction band and the Dy^{2+} $4f^{10}$ ground state is within 0.9 eV below. Following this concept, it is assumed that on exposure to photons of sufficient energy ($h\nu > 3.2$ eV; $\lambda < 390$ nm), the electron from Eu^{2+} is excited to the conduction band and

Eu^{3+} is formed. Since the Dy^{2+} ground state is within 1 eV below the conduction band, Dy^{3+} may trap such electron with about 1 eV binding energy [28]. Thermal release of that trapped electron and recombination with Eu^{3+} then yields the 5d–4f emission of Eu^{2+} as the persistent luminescence.

Fig. 4 shows TL glow curves for $SrAl_2O_4$: Eu, Dy powder phosphors prepared with x = 0.01, 0.02 and 0.03 ion doping of Dy^{3+}. The general nature of TL curves is similar in different cases: each curve peaks at a temperature around 145°C. It is observed that varying concentration of Dy does not affect the peak position much. However, the emission intensity is found to increase with increasing Dy concentration and for x = 0.02 molar ratio, the intensity is quenched [29] and decreases for further concentration (x = 0.03). The reason for such quenching may be the increase in probability of non-radiative transitions of the luminescent molecules from the excited state to the ground state in comparison to the probability of radiative transitions. The temperature dependence of TL intensity is represented in the following way [30]-

$$I = A\frac{p_{t0}}{\tau_{t0}}\exp\left(\frac{-E_t}{kT}\right)\exp\left[-\int_{T_0}^{T}\frac{1}{\beta\tau_{t0}}\exp\left(\frac{-E_t}{kT}\right)dT\right] \qquad (2)$$

where 'A' is a constant related to emission efficiency, p_{t0} - the initial density of trapped holes, τ_{t0} -the oscillation factor, E_t -the activation energy (trap depth), k -the Boltzmann constant, T_0 - the initial temperature and β is the temperature rise rate. In order to examine the effects of the auxiliary activator elements on the afterglow phosphorescence, the depth of the traps and the density of the trapped carriers are evaluated using the TL technique. Fig. 5 shows the variation of trap depth with temperature. The values of different parameters calculated from glow curves are presented in table 2. The value of trap depth, which resembles the activation energy [31], is calculated to lie between 0.47 and 0.49eV. For these glow curves the activation energy with maximum intensity using Chen method [32] is calculated to be 0.47 eV. These values are quite comparable with those calculated from initial rise method (fig. 5). It is worth reporting that the shape factor, which ranges from 0.51 to 0.53, shows the second order kinetics for prepared samples.

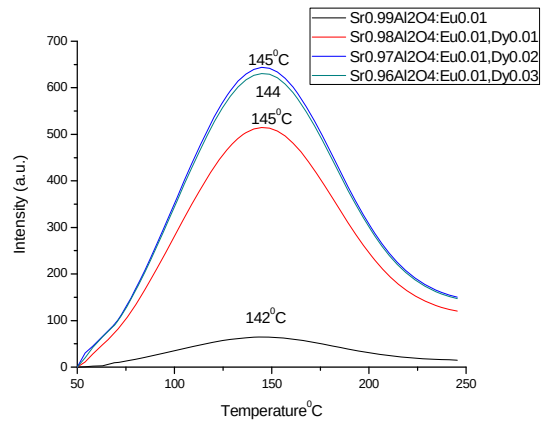

Fig.4 TL glow curves of $SrAl_2O_4$: Eu phosphors with different Dy concentrations

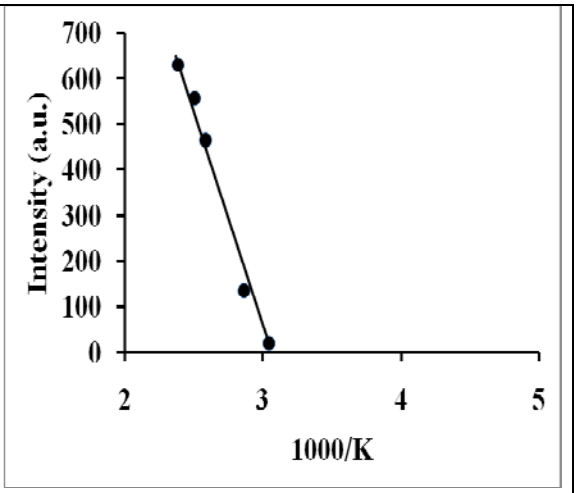

Fig.5 Variation of trap depth with temperature

Table 2 Values of different parameters calculated from TL glow curves

T_1 (°C)	T_m (°C)	T_2 (°C)	Peak parameters			Shape factor	Order of kinetics	Activation energy(eV)	Frequency factor(s^{-1})
			τ	δ	ω	μ= δ/ω			
97	142	193	45	51	96	0.53	2	0.49	1×10^7
98	145	194	47	49	96	0.51	2	0.48	5×10^6
97	144	196	47	52	99	0.52	2	0.48	6×10^6
97	145	196	48	51	99	0.51	2	0.47	4×10^6

4. Conclusions

Monoclinic samples of $SrAl_2O_4$ with varied dopant concentration of Dy have been successfully synthesized by CST, which proves to be a viable method in comparison to other existing techniques as it gives particles of smaller size. The SEM results present flake like structure of particles showing improvement with greater Dy concentration. The XRD results show variation in intensity with different volumes of Dy along with crystallite size lying in nano order. The TL glow curves are centered on a particular temperature with the help of which trap-depth, frequency factor and shape factor are calculated.

References

[1] S.K. Sharma, S.S. Pitale, M.M. Malik, M.S. Qureshi, R.N. Dubey, J. Alloy Compd. **482**, 468 (2009).
[2] J. Holsa, H. Jungner, M. Lastusaari, J. Niittykoski, J. Alloys Compd. **326**, 323 (2001).
[3] A. Nag, T.R.N. Kutty, J. Alloys Compd. **354**(1-2), 221 (2003).
[4] Y.H. Lin, Z.T. Zhang, F. Zhang, Z.L. Tang, Q.M. Chen, Mater. Chem. Phys. **65**(1), 103 (2000).
[5] Y. Murayama, N. Takeuchi, Y. Aoki, T. Matsuzawa, US Patent 5424006, (1995).
[6] Y.L. Liu, B.F. Lei, C.S. Shi, Chem. Mater. **17**, 2108 (2005).
[7] Y.H. Lin, Z.T. Zhang, Z.L. Tang, J.Y. Zhang, Z.S. Zheng, X. Lu, Mater. Chem. Phys. **70**(2), 156 (2001).
[8] Y.H. Lin, Z.T. Zhang, F. Zhang, Z.L Tang, Q.M. Chen, Mater. Chem. Phys. **65**, 103 (2000).
[9] L. Xiao, S. Meng, Z. Junying, W. Tianmin, J. Rare Ear. **28**(1), 150 (2010).
[10] M.D. Segall, P.L.D. Lindan, M.J. Probert, C.J. Pickard, P.J. Hasnip, S.J.Clark, M.C. Payne, J. Phys: Cond. Mater. 14, 2717 (2004).
[11] T.Y. Peng, H.J. Liu, H.P. Yang, C.H. Yan, Mater. Chem. Phys. **85**, 68 (2004).
[12] C.H. Lu, S.Y. Chen, C.H. Hsu, Mater. Sci. Engg. B **140**, 218 (2007).
[13] T.Y. Peng, H.P. Yang, X.L. Pu, B. Hu, Z.C. Jiang, C.H. Yan, Mater. Lett. **58**, 352 (2004).
[14] Z.L. Fu, S.H. Zhou, Y.N. Yu, S.Y. Zhang, Chem. Phys. Lett. **395**, 285 (2004).
[15] Y.F. Xu, D.K. Ma, M.L. Guan, X.A. Chen, Q.Q. Pan, S.M. Huang, J. Alloys Comp. **502**, 38 (2010).
[16] R. Zhang, G. Han, L. Zhang, B. Yang, Mat. Chem. Phy. **113**, 255 (2009).
[17] J.C. Toniolo, M.D. Lima, A.S. Takimi, C.P. Bergmann, Mat. Res. Bull. **40**, 561 (2005).
[18] D. Ravichandran, S.J. Johnson, S. Erdei, R. Roy, W.B. White, Displays **19**, 197 (1999).
[19] S.H.M. Poort, W.P. Blokpoel, G. Blasse, Chem. Mater. **7**, 1547 (1995).
[20] T. Minami, Y. Kuroi, H. Yamada, S. Takata, J. Sid. **6**/1, 17 (1998).
[21] N.M. Son, L.T.T. Vien, L.V.K. Bao, T.N. Ngoc, J. Phys.: Conference Series **187**, 012017 (2009).
[22] S.K. Sharma, S.S. Pitale, M.M. Malik, V. Gundurao, S. Chawla, M.S. Qureshi, R.N. Dubey, J. Lum. **130**, 240 (2010).

[23] A.V. Feitosa, M.A.R. Miranda, J.M. Sasaki, M.A. Arujo-Silva, Braz. J. Phys. **34**(2B), 656 (2004).
[24] A.U. Ubale, V.S. Sangawar, D.K. Kulkarni, Bull. Mat. Sci. **30**(2), 147 (2007).
[25] K.S. Hwang, B. Kang, S. Daikim, S. Hwangbo, J.T. Kim, Bull. Mat. Sc. **34**(5), 1059 (2011).
[26] M. Avdeev, S. Yakolev, A. Yaremchenko, V. Kharton, J. Sol. Stat. Chem. **180**(12), 3535 (2007).
[27] L.M. Ruben, F. Masayoshi, T. Hiroaki, T. Minoru, Mater. Lett. **61**, 756 (2007).
[28] A.J.J. Bos, R. M. V. Duijvenvoorde, E. V. Kolk, W. Drozdowski, P. Dorenbos, J. Lumin. **131**, 1465 (2011)
[29] G.C. Mishra, A.K. Upadhyay, S.K. Dwiwedi, S.J. Dhoble, R.S. Kher, J. Mat. Sc. **47**(6), 2752 (2012).
[30] Z. Zhou, W. Luo, B. Lu, X. Wu, Opto. Adv. Mater. **5**, 125 (2011).
[31] N.M. Son, L.T.H. Vien, L.V.K. Bao, N.N. Trac, J. Phys.: Con. Series **187**, 012017 (2009).
[32] K. V. Eeckhout., P. F. Smet, D. Poelman, Materials **3**, 2536 (2010).